Design of a Controller for a Linear Drive of a Magnetic Levitating Transportation Vehicle

D. Brakensiek, H. Bornefeld, and G. Henneberger

Department of Electrical Machines (IEM)
Aachen Institute of Technology (RWTH)
Schinkelstraße 4, D-52056 Aachen, Germany
phone: +49 241 80-97636 – fax: +49 241 80-92270 – e-mail: Dirk.Brakensiek@iem.rwth-aachen.de

***Abstract* – This paper deals with the design of a control system for a linear drive. The drive comes into operation at an autonomous transportation vehicle. The vehicle is equipped with a magnetic levitation system and optionally supplied by a contactless energy- and information transmission.**
The control system consists of a closed-loop position control with inner speed control loop and current control loop. The commercial software *Matlab/Simulink* was used to design the control system. A *dSPACE* DSP controller board executes the controller application. A driving program guides the vehicle at different speeds to various positions.
After mentioning the results of the FEM calculations of the motor, the paper describes the structure of the control system, the creation of a real-time-process and gives examples for the driving performance at the test bench.

1. Introduction

A magnetic levitating vehicle combined with a linear drive offers many advantages, such as high velocity, no wear and no maintenance. Therefore it provides a high reliability. Possible applications are conveyor systems for clean rooms or for food industry or luggage transportation systems at airports. Because of the high velocity the time e.g. between an arriving flight at an aiport and the connection flight can be halved. In the same way personnel costs for maintenance can be reduced significantly.

2. The Transportation System

The vehicle consists of a bogie and a luggage shell with a propulsion and levitation head on each corner of the bogie. A short-stator type linear homopolar motor has been chosen [1]. The levitation magnet is U-core shaped and hybrid excited. Permanent magnets compensate the static load of the vehicle, the current in the coils stabilizes the magnet in its working point. The levitation air gap is set according to the load of the vehicle in a way that the current is minimized [2]. In order to obtain higher reluctance forces for the lateral guidance the reaction rail is slotted. The power converters for levitation and propulsion are mounted on the vehicle. Eddy current sensors detect the levitation air gap. Three light barriers at each corner are used to detect the position of the vehicle at regular intervals of 10 mm. Every propulsion head has its own position encoder.

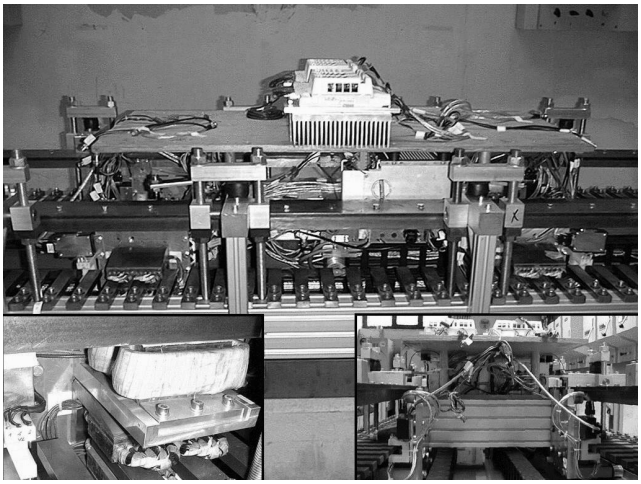

Fig. 1. The transportation system.

The track consists of two passive rails, one for levitation and lateral guidance and one for propulsion. The energy- and information transmission lines will be situated below the motor. The motor itself is located below the levitation system. Fig. 1 displays the transportation system.
Because of the principle of motor, bearing magnets and energy- and data transmission the transportation system has no wear and therefore requires no maintenance. The passive tracks are cheap and easy to build.

3. The Homopolar Motor

The principle of the homopolar motor is shown in Fig. 2. Two rare-earth permanent magnets generate the excitation flux. The flux is guided by the flux concentrating pieces in the track and closes through the armature and the yoke.

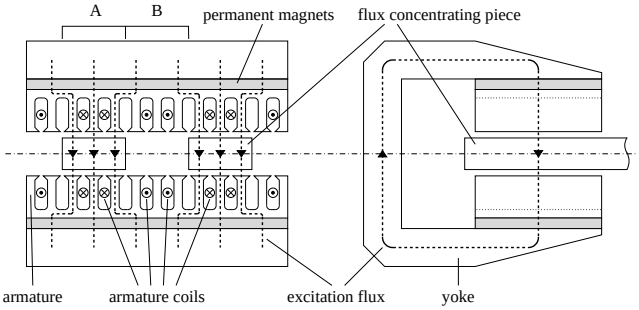

Fig. 2. Principle of the homopolar motor.

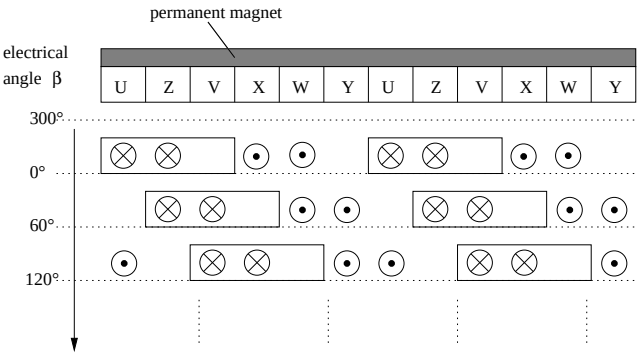

Fig. 3. Field-oriented supply of the armature windings.

As a result the flux density under pole A is high whereas it is low under pole B. If the armature coils, designed as a conventional travelling-field winding, are fed with field-orientated current the propulsion force under pole A is high whereas it is low in the opposite direction under pole B due to the modulation of the flux density. The resulting force acts into the driving direction. The armature coils are fed with square-wave currents: The positive and the negative phase-currents with a length of 120° electrical each are separated by a zero current with a length of 60° electrical. So every 60° the current commutates to the next phase, Fig. 3. Though the airgap is large the motor achieves a high efficiency.

4. Calculation of the Forces

To calculate the forces of the motor a three-dimensional finite-element-model was built [3], [4]. The model, built using the FEM-Program Ansys, consists of about 455 000 elements and 77 000 nodes. Fig. 4 shows the magnetic induction on the surface of the homopolar motor at rated load. The flux concentration due to the iron elements is visible very clearly within the teeth of the armature. The results of the propulsion force calculation at rated load and no-load, called cogging force, are depicted in Fig. 5. The propulsion force at load comprises two parts, the reluctance force with a force ripple of $\pm 30\,N$ and the current generated force, providing low deviations. As a result of a vertical displacement

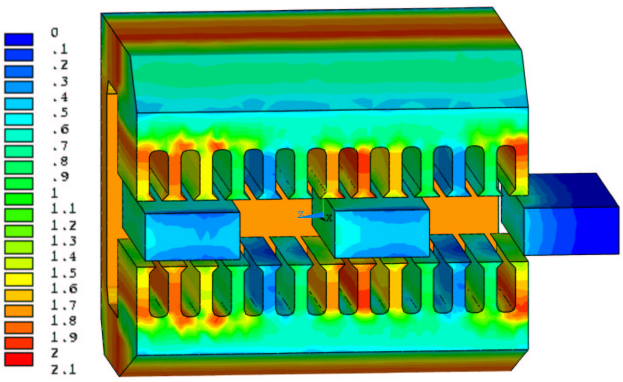

Fig. 4. Magnetic induction on the surface at load.

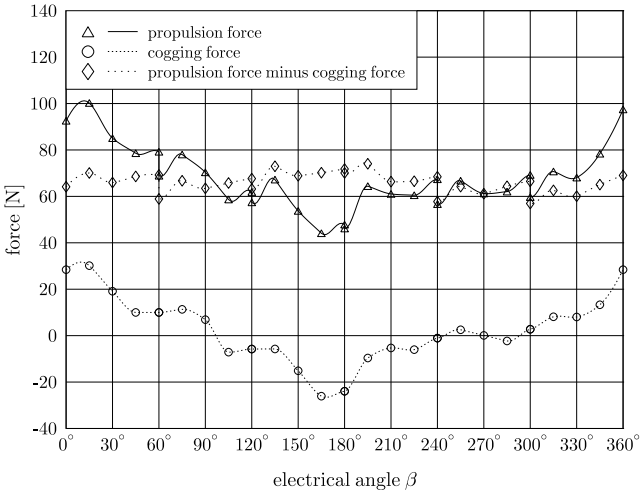

Fig. 5. Propulsion force at rated load and no-load.

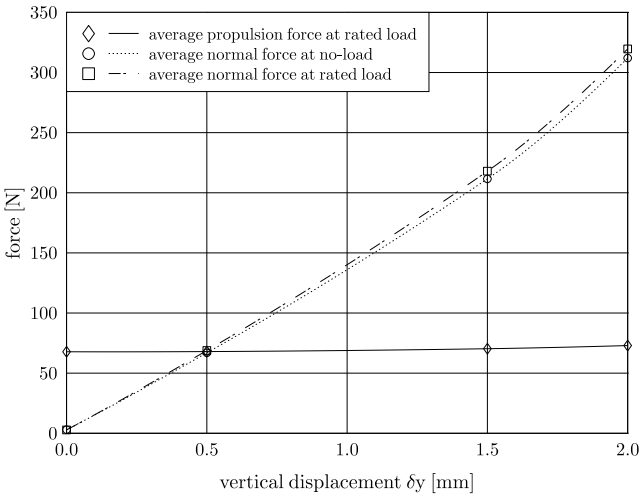

Fig. 6. Average normal- and propulsion force.

of the motor, i.e. upper air gap is not equal to lower air gap, normal forces approximately linear to the vertical displacement are created whereas the propulsion force remains constant, Fig. 6.

5. The Test Bench

The test bench consists of two parts, the vehicle with the track and the control interface. The controller application is executed on the DSP board and influenced by an operator via the PC. The position sensor signals are submitted to the DSP board using an electrical isolation. The controller algorithm switches the currents in the motor. The actual current is measured by a current transformer and also submitted to the DSP. The structure of the test bench is displayed in Fig. 7.

6. The Structure of the Controller

Fig. 8 shows the structure of the control system of the drive. The inner loop contains the current controller, the outside loops are the speed and position controller. The position and the speed controller are realised as PI controllers with out-

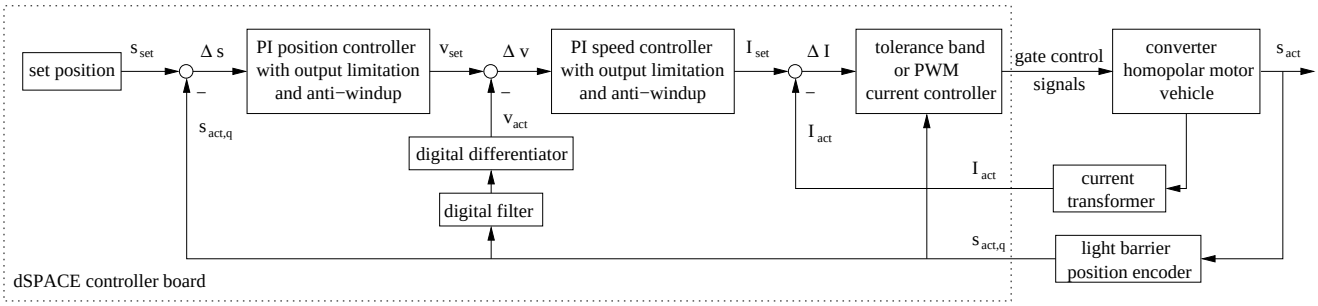

Fig. 8. Structure of the control system.

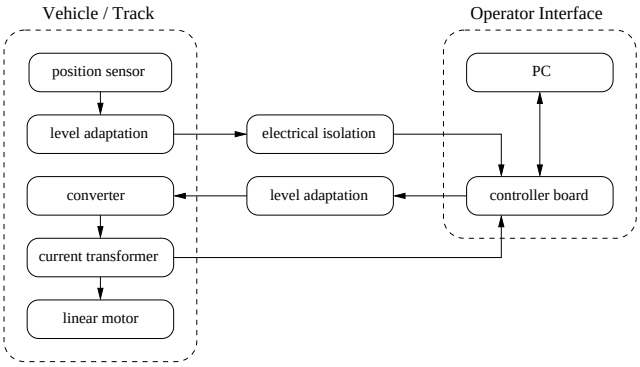

Fig. 7. Structure of the test bench.

put limitation and anti-windup loop. The current controller can be implemented as a tolerance band controller or as a puls-width modulation current controller. The performance of both is comparable, but using the puls-width modulation current controller the resulting noise produced by the motor is less than using the tolerance band current controller. The position of each linear motor is detected by three light barriers in steps of 10 mm, which corresponds to an electrical angle of 60°. This position signal is filtered and the first derivative is used to obtain the actual speed v_{act}. The filter chosen is a 2nd order lowpass butterworth filter with a cut-off frequency of 10 Hz. The position signal is required also for the field-oriented control of the current.

The controllers, the generation of the setpoint value of the position, the filter and the differentiator are implemented within the software on the controller board. Inputs to the controller board are the position encoder signals and the actual current I_{act}, outputs are the gate control signals for the IGBT converter. As many parts as possible are realised within the software to achieve a great flexibility.

The structure of the position and the speed PI controller is displayed in Fig. 9. If the values between input and output of the output-limiter differ, the anti-windup gain reduces the integral part of the controller. This means, that anti-windup takes effect, when the output is limitated, e.g. at the beginning of a setpoint step-change. As a consequence of this an overshot of the controlled variable can be reduced. The behaviour of the system becomes more dynamic.

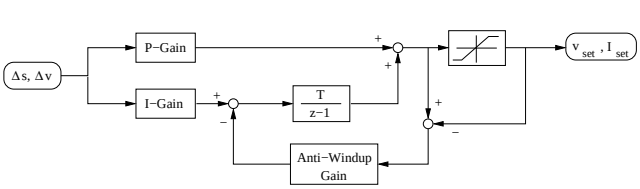

Fig. 9. The PI controllers with output limitation and anti-windup.

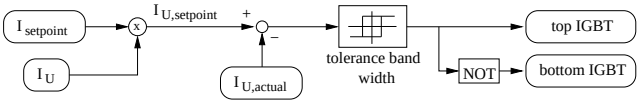

Fig. 10. The tolerance band controller for 1 phase.

The design of the tolerance band current controller is depicted in Fig. 10. The amplitude of the current setpoint value, $I_{setpoint}$, is multiplied with $+1, 0$ or -1, I_U, to get the current setpoint value of the respective phase, $I_{U,setpoint}$, according to the actual position. The current control deviation is compared with the width of the tolerance band. This block switches the top and the bottom IGBT of one half-bridge of the three-phase bridge on and off to achieve the desired current.

The reference input variable, e.g. the setpoint value of the position, is created by a driving program. The user can define any desired driving cycle with different stop positions and velocities.

7. Real-Time-Process

The creation of a real-time-process is explained in Fig. 11. At the first step a model of the control system is constructed using *Matlab/Simulink*. In this state the model can be tested in a simulation. The *dSPACE* Real-Time-Workshop contains the libraries for the input and output interfaces of the controller board. It compiles the model to a code executable on the controller board. After that the user designs a control and visualization panel using the software *Control Desk*. The variables of the model can be influenced by the created control panel. Also variables, e.g. the velocity, can be plotted on the screen.

In the same manner the user can influence the controller board application variables by the libraries *MLIB/MTRACE*. By the use of these libraries a driving program was created.

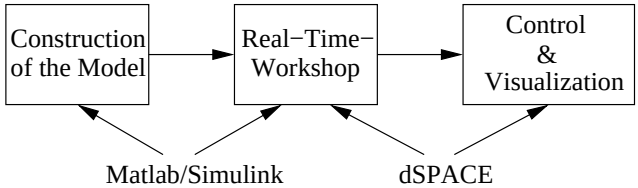

Fig. 11. Creation of a real-time-process.

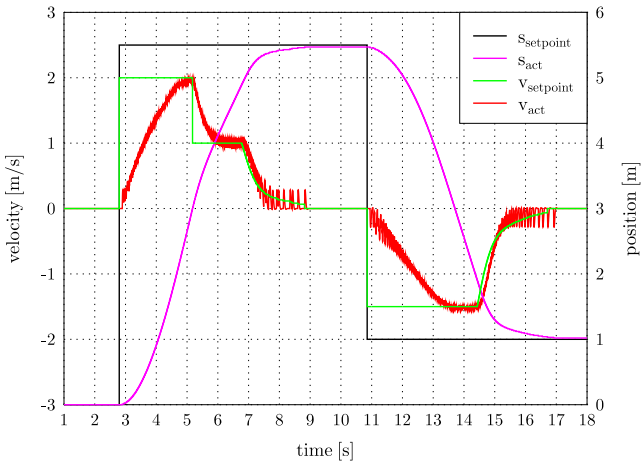

Fig. 12. Driving performance of the control system.

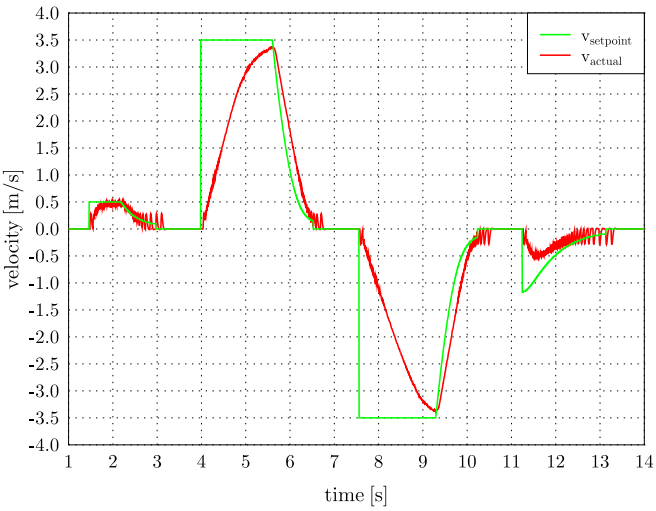

Fig. 13. Performance after optimisation.

So working with the controller board offers the following advantages:

- Large number of various digital and analog inputs and outputs
- Comfortable programming environment
- Good arithmetic performance (real-time)
- Possibility of taking measured data

8. Results

The first results of the driving at the test bench are shown in Fig. 12. In this case only the two motors are used. The user may define any driving cycle with various positions and velocities. Every state in a cycle consists of a set position, a maximum velocity to drive the vehicle to this position and a period of time for which the vehicle remains at the position. As well the vehicle can change its set velocity while driving. In this special case the vehicle changes the velocity while driving to the position $5.5\,m$ with a maximum velocity of $2\,m/s$ to $1\,m/s$ at a position of $3\,m$. The vehicle remains at its destination for $2\,s$ and drives back to the position $1\,m$ with a velocity of $1.5\,m/s$. The velocity pulses at slow speeds arise due to the coarse resolution of the position encoder. Also because of this the controllers are turned off, if the position error is less than $\pm 35\,mm$.
Further optimisations lead to the results displayed in Fig. 13. In comparison with the results in Fig. 12 four motors are used. The current is now limited to the 2.5-fold nominal current. In the end the parameters of the position controller are optimised. At a distance of $5\,m$ for accelerating and retarding the maximum velocity is now $3.3\,m/s$. The acceleration was increased from $a = 1.14\,m/s^2$ to $a = 3.13\,m/s^2$.

9. Conclusion

The implementation of the control system for the linear drive using the controller board and the corresponding software offers a very comfortable programming environment. The interfaces between software controller and controlled system are easy to operate. The realisation of algorithms within software gives a great flexibility in the control system design. Using a driving program as general as possible the vehicle is able to drive to various positions with a driving performance meeting the demands perfectly. Now algorithms will be developed to drive the vehicle through horizontal curves.

References

[1] W. Evers, *Entwicklung von permanenterregten Synchronlinearmotoren mit passivem Sekundärteil für autonome Transportsysteme*, Dissertation, Fakultät für Elektrotechnik und Informationstechnik der RWTH Aachen, Verlag Shaker, 2000.

[2] I. Gröning, *Magnetische Lagerung für ein autonomes Transportsystem mit normalkraftbehaftetem Linearantrieb*, Dissertation, Fakultät für Elektrotechnik und Informationstechnik der RWTH Aachen, Verlag Shaker, 2000.

[3] W. Evers, G. Henneberger, H. Wunderlich, A. Seelig, "A linear homopolar motor for a transportation system," in *Proceedings of the 2nd International Symposium on Linear Drive for Industry Applications (LDIA 1998)*, Tokyo, Japan, 1998, pp. 46–49.

[4] D. Brakensiek, G. Henneberger, "Design of a Linear Homopolar Motor for a Magnetic Levitating Transportation Vehicle," in *Proceedings of the 3rd International Symposium on Linear Drives for Industry Applications (LDIA 2001)*, Nagano, Japan, 2001, pp. 352–355.